

Grundlagen der Biomechanik – 719.009

Sommersemester 2016, TU Graz

Vortragende:

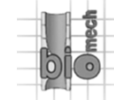
Gerhard A. Holzapfel
Justyna A. Niestrawska

Studienassistentin:

Julia Branstetter



Institut für Biomechanik
Stremayrgasse 16/2, TU-Graz

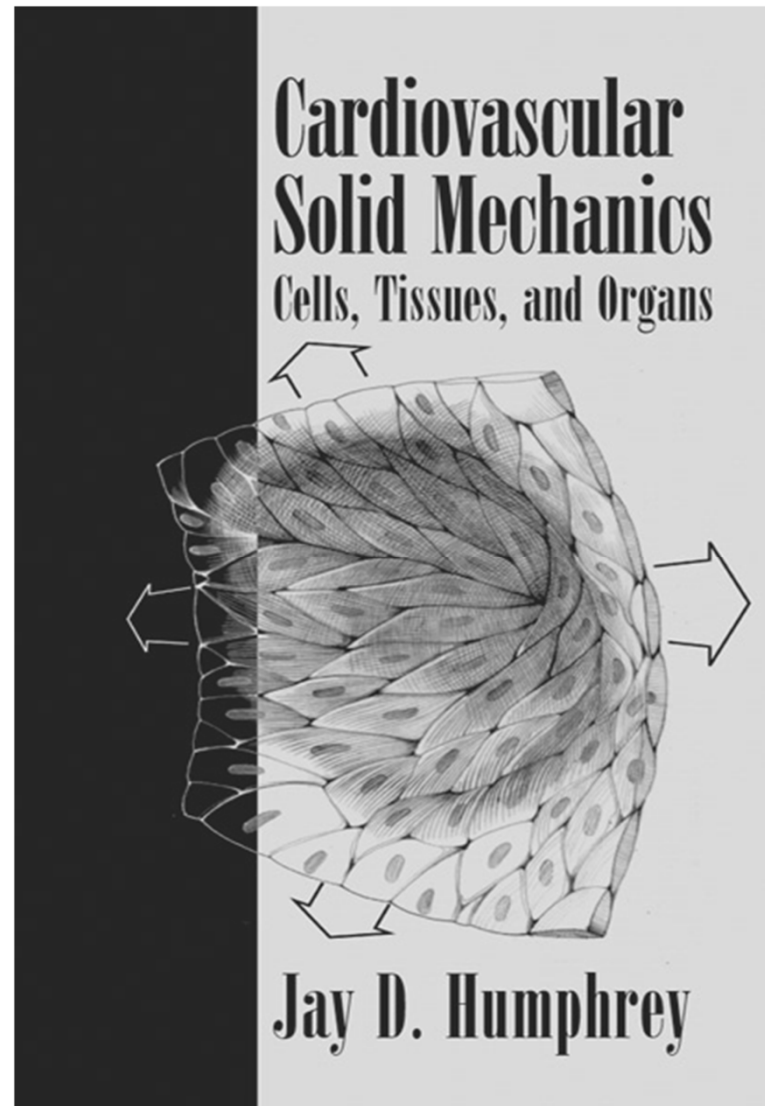


Vorlesung –18:

Arterial Wall Mechanics

- **Finite Deformations, Anisotropy**
- **Reference Configuration, Residual Stress**
- **Active Response**

Literature



Humphrey (2002)

Recall general characteristics of soft tissue

- Elastic
- Nonlinear
- Heterogeneous
- Incompressible
- Anisotropic

For arteries additionally:

- Residual stresses
- Active response

See - heart,
- reinforced concrete

- Helps to balance forces
- Controls remodeling (growth
generates residual stresses)
- Required for zero stress state

See - heart muscle,
- skeletal muscle

Recall general characteristics of soft tissue

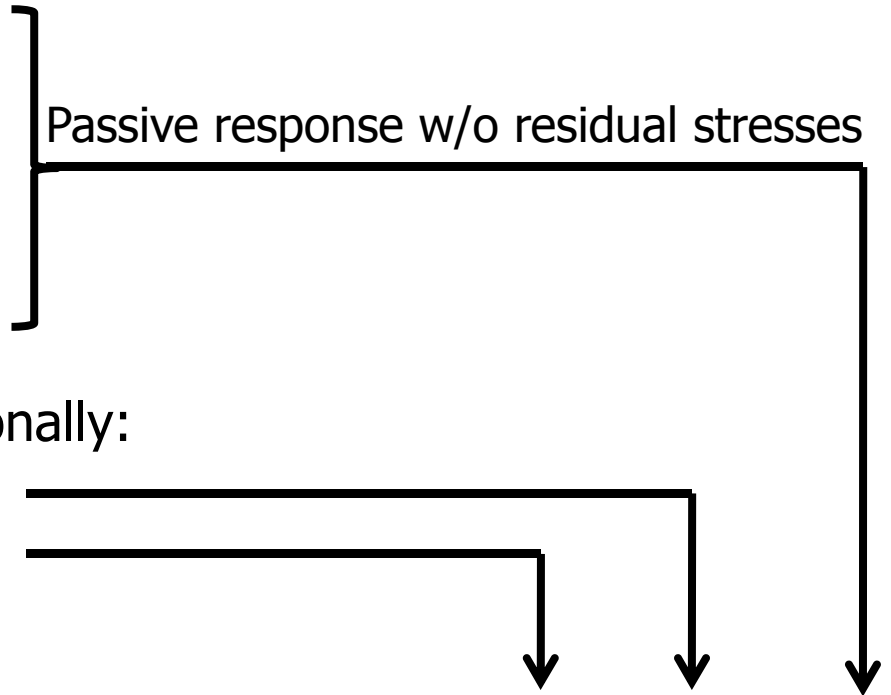
- Elastic
- Nonlinear
- Heterogeneous
- Incompressible
- Anisotropic

Passive response w/o residual stresses

For arteries additionally:

- Residual stresses
- Active response

Cauchy stress $\sigma = \sigma^a + \sigma^r + \sigma^p$



Finite Deformations, Anisotropy

Delineation of deformations experienced by an artery, under conditions of interest, is essential for both establishing an appropriate theoretical framework and guiding *in vitro* experimental studies of the constitutive behavior.

In addition to the finite residual stretches in unloaded arteries, most arteries are significantly stretched in the axial direction in the *in vivo* state, e.g. carotid artery approx. 50-70% in canines, rabbits, and rats.

The extend of axial retraction varies with position → Deng et al (1994) report a variation in aortic retraction in rat aorta from 20% in and near the arch to 50% in the abdominal region.

Han and Fung (1995) reported detailed measurements of the *in situ* axial stretch λ^* (at zero blood pressure) in porcine and canine aorta as a function of position.

They show that λ^* increases nonlinearly from about 1.2 in or near the arch to 1.6 near the aorto-iliac bifurcation. They also measured the cross-sectional area A^* as a function of location, and showed that

$$\lambda^* \left(\frac{x}{L} \right) = \alpha - \beta \left(\frac{A^*(x/L)}{A_0} \right) \quad x \in [0, L]$$

- L ... Total length of the aorta from the aortic root to the aorto-iliac bifurcation
- α and β ... Parameters. Values are approximately 1.6 and 0.25
- A_0 ... Mean cross-sectional area of the aorta

In the aorta λ^* is larger in regions where A^* is less.

Han and Fung estimated the axial force needed to restore the aorta to its *in situ* length to be $\sim 0.88\text{N}$.

Additional *in vivo* axial extensions result from limb motion, for example 20% extensions in human popliteal arteries due to knee flexion and 20% to 60% extension in canine carotids due to cervical (Hals) extension.

Blood pressure-induced axial extensions tend to be small (e.g. 1% in the descending aorta) except in the pulmonary arteries and ascending aorta where they can be 5% to 11%.

There are few reports on the *in vivo* circumferential extension.

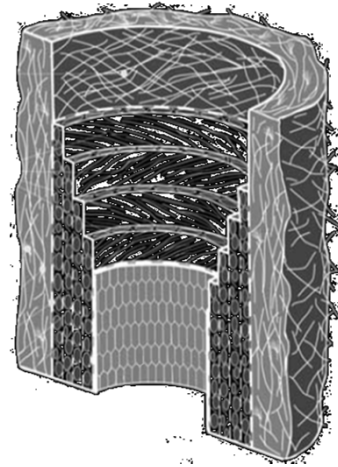
Canine carotid artery is reported to be circumferentially extended 57% at 100 mmHg *in vivo*.

Changes in diameter from diastole and systole can be 10% to 15% in the pulmonary artery, 6% to 10% in carotids, but only 2% to 5% in the aorta (Dobrin, 1978).

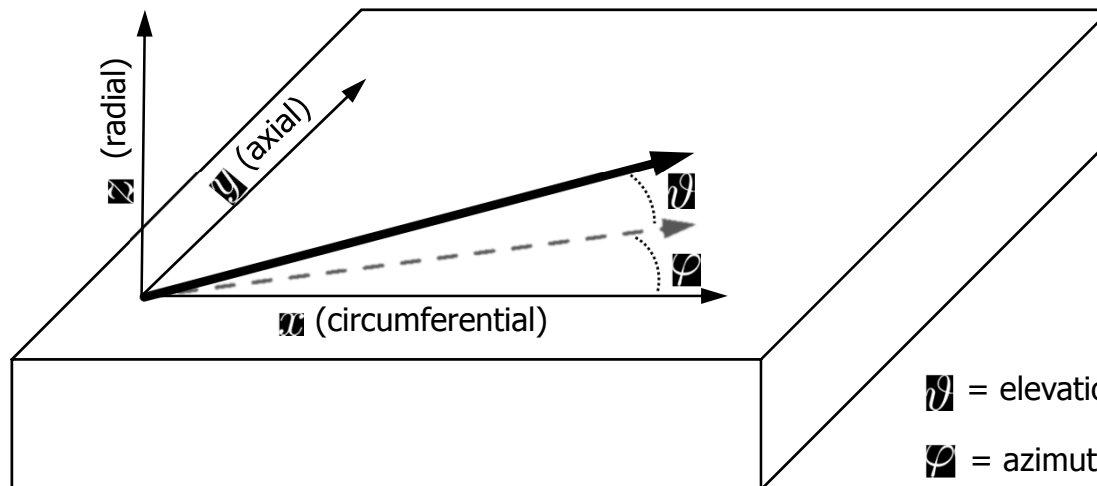
Arteries experience finite deformations *in vivo*.

Measurement of collagen fiber directions in the aorta

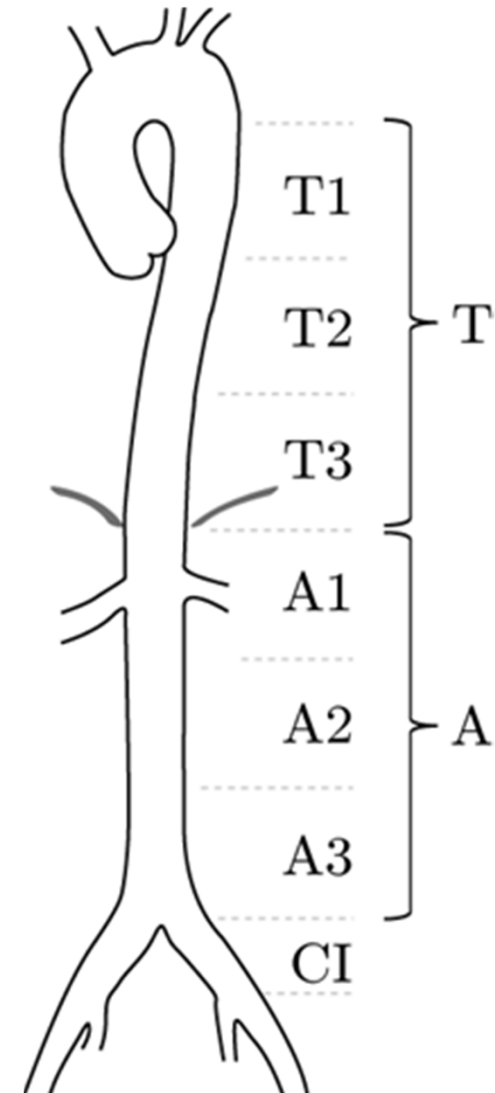
Work of A. J. Schriefl



Holzapfel et al. [*J. Elasticity*], (2000)



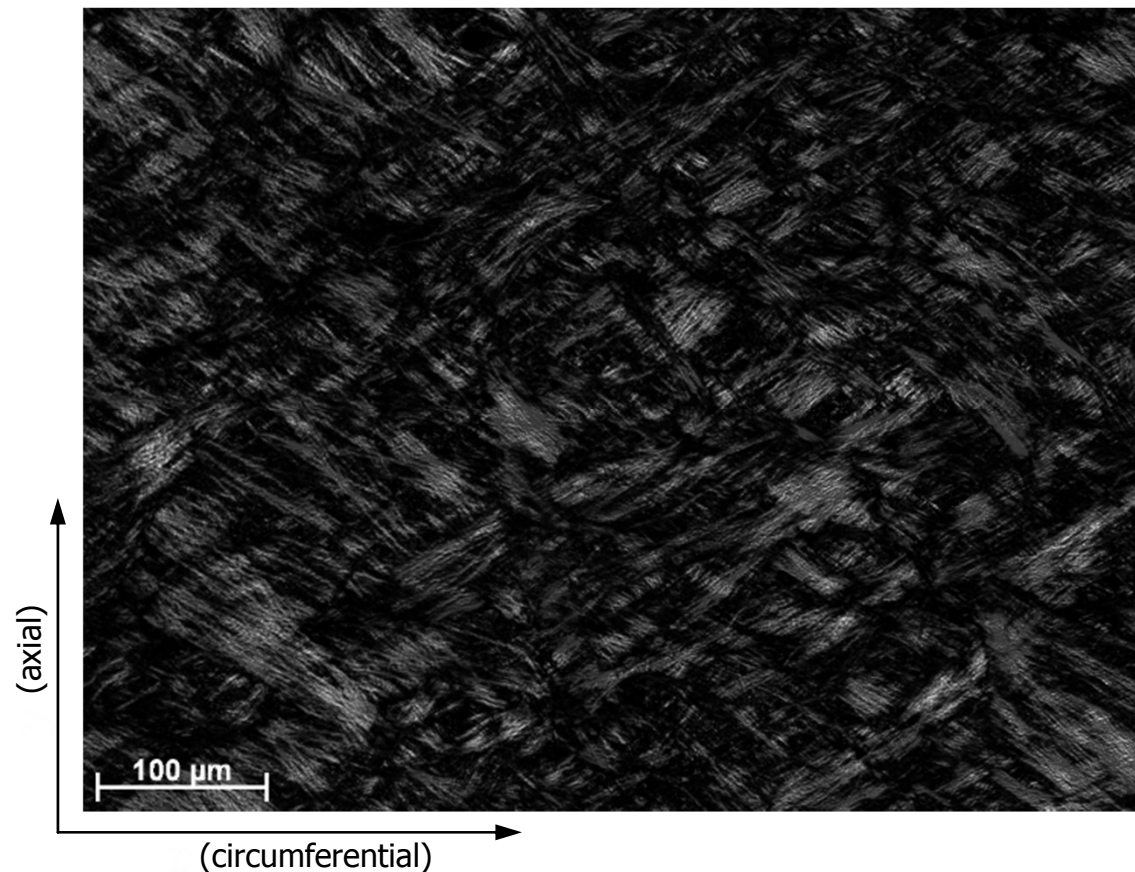
= elevation angle
 = azimuthal angle



Measurement of collagen fiber directions in the aorta

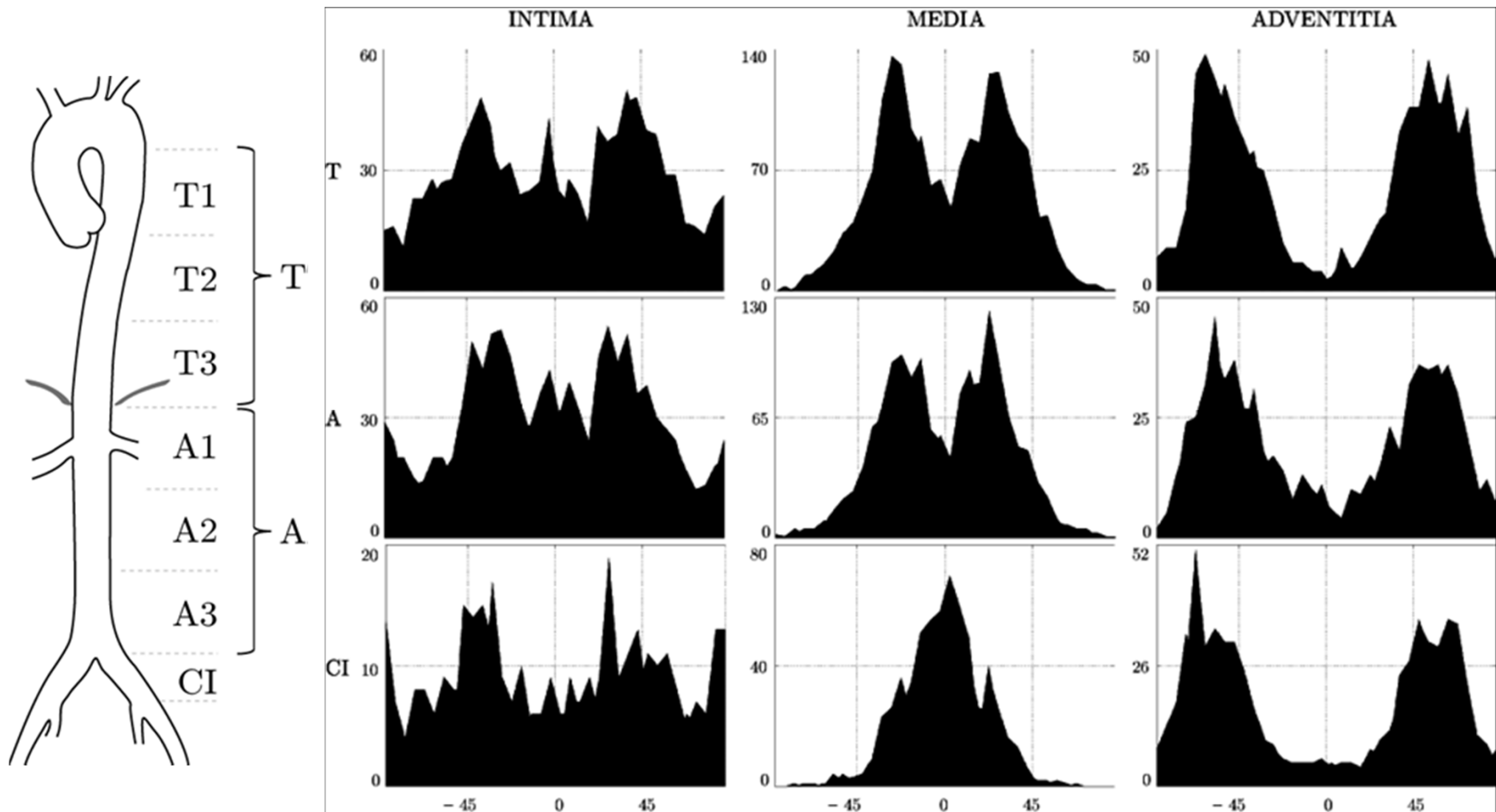
Collagen fibers in the intimal wall at location T2

- Representative image taken with polarizing microscope
- Notice two distinct fiber families



Measurement of collagen fiber directions in the aorta

Overview of the azimuthal angle



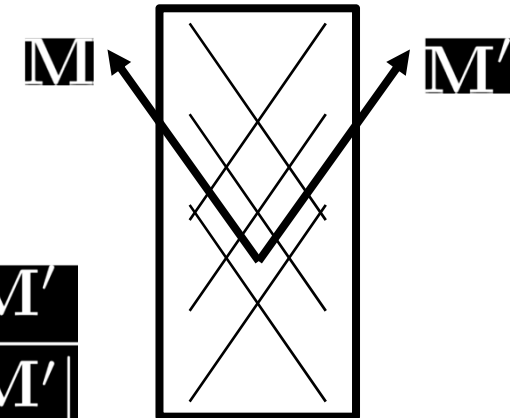
Measurement of collagen fiber directions in the aorta

	Location	No. of fiber families	Φ	SD	Θ	SD
Intima	T	2-4	$\pm 39^\circ$	17°	0°	9°
	A	2-4	$\pm 33^\circ$	16°	0°	9°
	CI	2-3	$\pm 40^\circ$	16°	0°	9°
Media	T	2	$\pm 25^\circ$	15°	0°	9°
	A	2	$\pm 21^\circ$	15°	0°	9°
	CI	1	0°	20°	0°	9°
Adventitia	T	2	$\pm 55^\circ$	17°	0°	9°
	A	2	$\pm 55^\circ$	19°	0°	9°
	CI	2	$\pm 55^\circ$	18°	0°	9°

- Approximately no elevation angle
- Mostly two fiber families
- Fibers in media more circumferentially directed

Modeling arterial tissue: A fiber reinforced fabric with two symmetric families of fibers

Holzapfel, Gasser, Ogden [J Elasticity], 2000



Cauchy-Green tensors $\mathbf{C} = \mathbf{F}^T \mathbf{F}$ $\mathbf{b} = \mathbf{F} \mathbf{F}^T$

Fiber directions $\mathbf{m} = \frac{\mathbf{F} \mathbf{M}}{|\mathbf{F} \mathbf{M}|}$ $\mathbf{m}' = \frac{\mathbf{F} \mathbf{M}'}{|\mathbf{F} \mathbf{M}'|}$

Invariants $I_1 = \text{tr} \mathbf{C}$ $I_4 = \mathbf{M} \cdot \mathbf{C} \mathbf{M}$ $I_6 = \mathbf{M}' \cdot \mathbf{C} \mathbf{M}'$

Strain-energy function

$$\Psi = \frac{c}{2} (I_1 - 3) + \frac{k_1}{2k_2} \sum_{i=4,6} \{ \exp[k_2 (I_i - 1)^2] - 1 \}$$

Cauchy stress

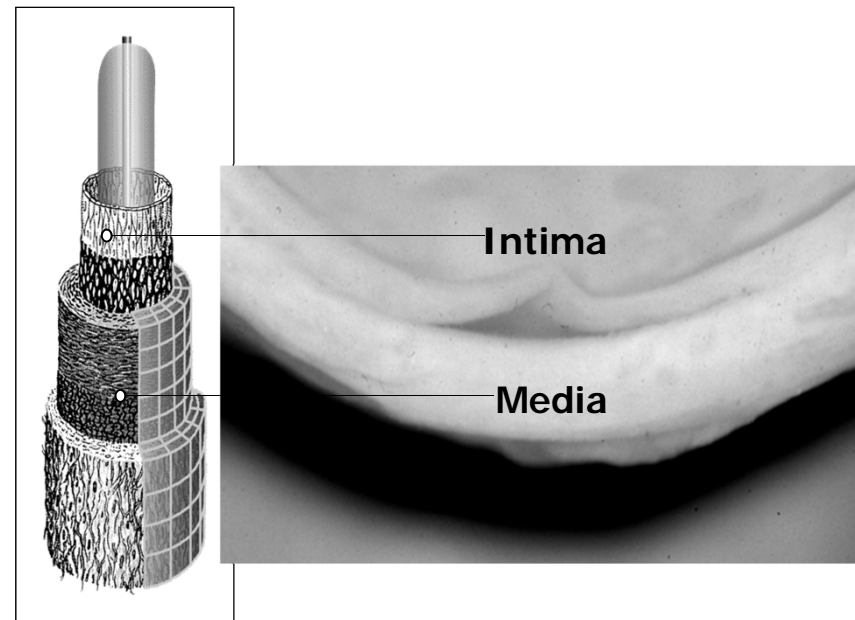
$$\boldsymbol{\sigma}^p = -p \mathbf{I} + 2 \frac{\partial \Psi}{\partial I_1} \mathbf{b} + 2 I_4 \frac{\partial \Psi}{\partial I_4} \mathbf{m} \otimes \mathbf{m} + 2 I_6 \frac{\partial \Psi}{\partial I_6} \mathbf{m}' \otimes \mathbf{m}'$$

Reference Configuration, Residual Stresses

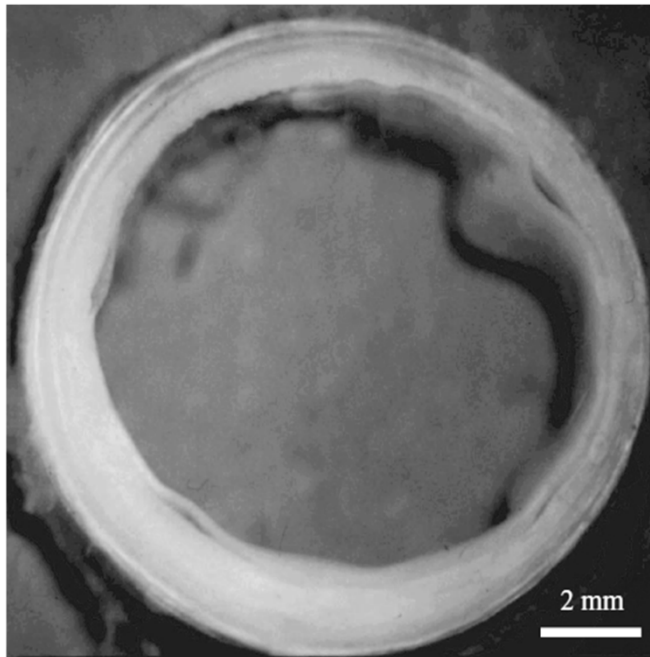
Identification of appropriate reference configurations is essential for the definition of stress, strain, stiffness, and material symmetry, thus essential to constitutive formulations and stress analyses.

For an elastic solid we ideally seek a single “natural” configuration, i.e. stress-free configuration, to which the material will return following any reversible (cyclic) process.

For a long lapse of time, the existence of a single natural configuration will be unlikely, due to growth, remodeling, aging, become diseased (Fung, 1973) → sequence of natural configurations.



Residual stress is the stress that exists in a body in the absence of externally applied loads.



Spontaneous buckling and delamination of the intima of an fresh human iliac arterial ring

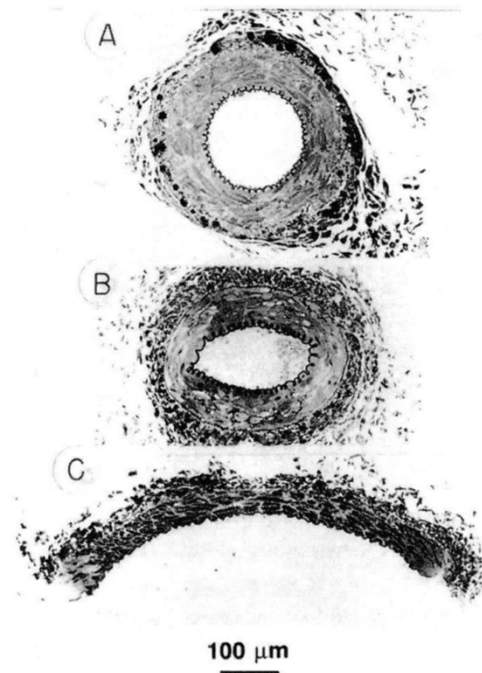


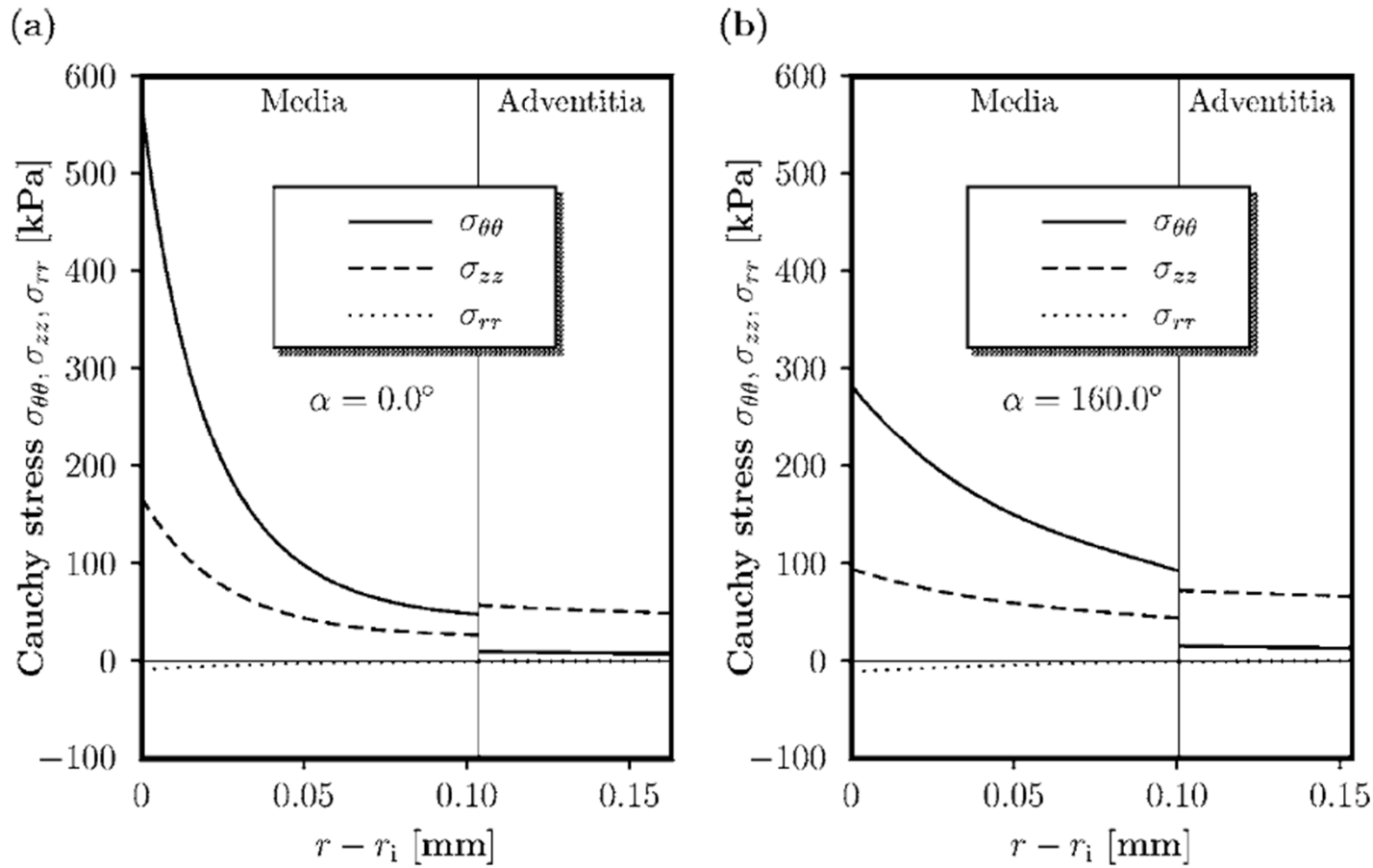
FIGURE 7.10. Light micrographs of arterial cross sections fixed in a 120 mm Hg (a), a no-load (b), and a radially cut, “stress-free” configuration (c). Note the increased waviness in the internal elastic lamina (black) in the unloaded ring, which is consistent with the existence of compressive residual stresses in the inner wall in this configuration. (From Fung and Liu, 1992, with permission.)

Humphrey (2002)

TABLE 7.2. Circumferential residual stretch ratios at the inner and outer surfaces of various excised, intact, unloaded arteries

Artery	Λ_0 , Intima	Λ_0 , Adventitia	Reference
Bovine aorta	0.904	1.102	Vaishnav & Vossoughi (1987)
Porcine aorta	0.923	1.078	Vaishnav & Vossoughi (1987)
Rat ileal	0.79	1.13	Fung & Liu (1992)
Rat plantar	0.66	1.16	Fung & Liu (1992)
Rat pulmonary	0.70	1.28	Fung & Liu (1992)
Rat saphenous	0.852	1.17	Fung & Liu (1991)
Rat pulmonary	0.908	1.11	Fung & Liu (1991)
Rat saphenous (d)	0.750	1.29	Liu/Fung (1992)
Rat pulmonary (d)	0.766	1.25	Liu/Fung (1992)
Rat a. aorta	0.956	1.08	Xie et al (1995)
Rat t. aorta	0.973	1.05	Xie et al (1995)
Dog carotid	0.83	1.14	Takamizawa & Hayashi (1987)

d, diabetic animal.



Stresses through the deformed layers media and adventitia at physiological state ($p=13.3$ kPa). From Holzapfel (2000)

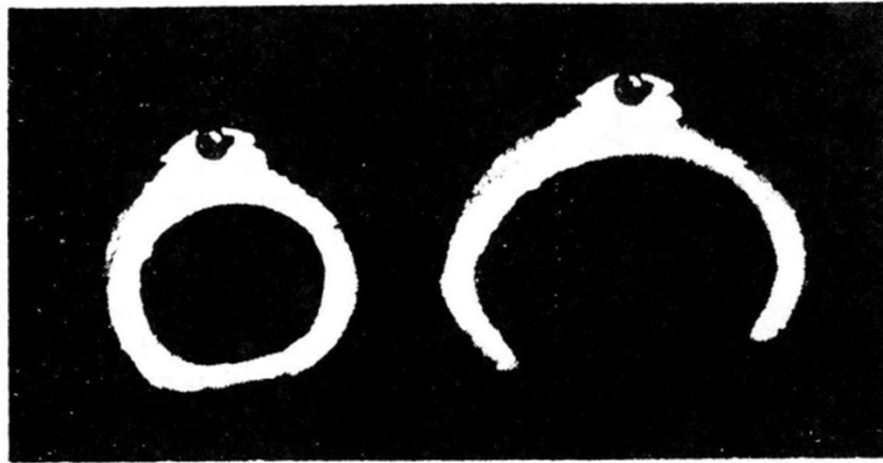
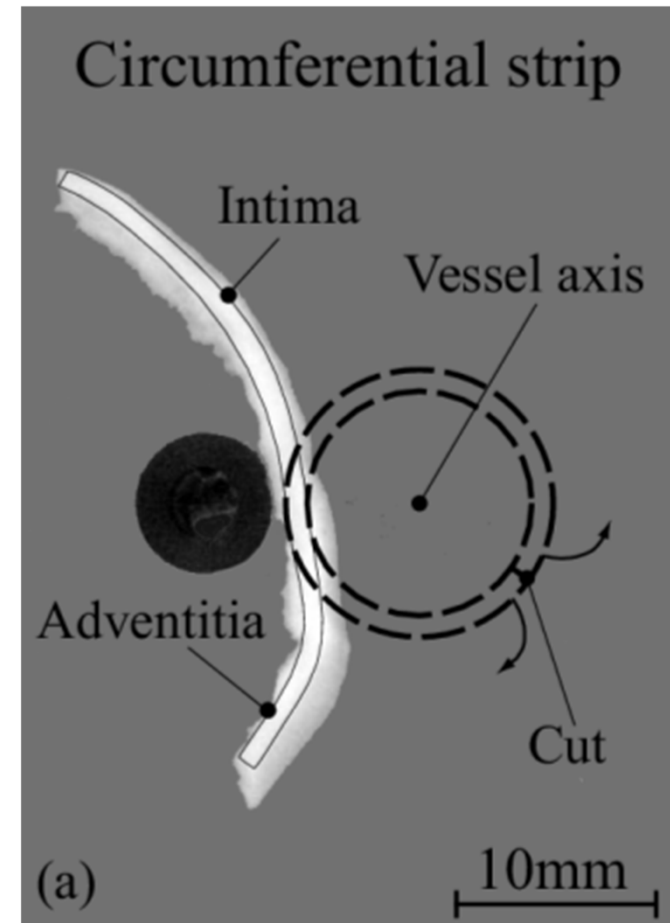
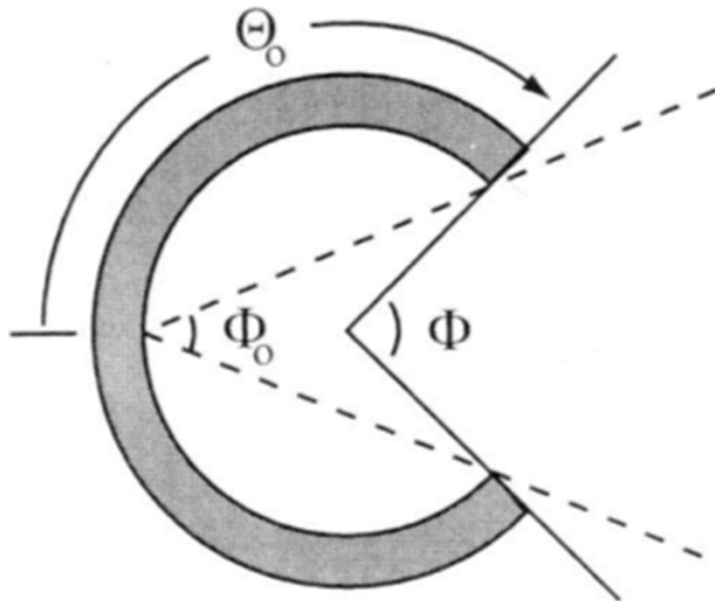


FIGURE 7.9. The “opening up” (right) of an originally unloaded intact arterial ring (left) following the introduction of a radial cut. (From Fung, 1984, with permission.)

Humphrey (2002)

Saini et al (1995) showed, using selective digestion of different components of the arterial wall, that elastin appears to be responsible for much of the residual strain in the normal wall.





Chuong and Fung (1986) suggested that an “opening angle” Θ_0 can serve as a single measure of the residual strain.

FIGURE 7.12. Schema of an opened arterial ring, and its quantification via the opening angle Θ_0 . Note, too, the use of other metrics including $\Phi = 2(\pi - \Theta_0)$ and $\Phi_0 = (\pi - \Theta_0)$.

Humphrey (2002)

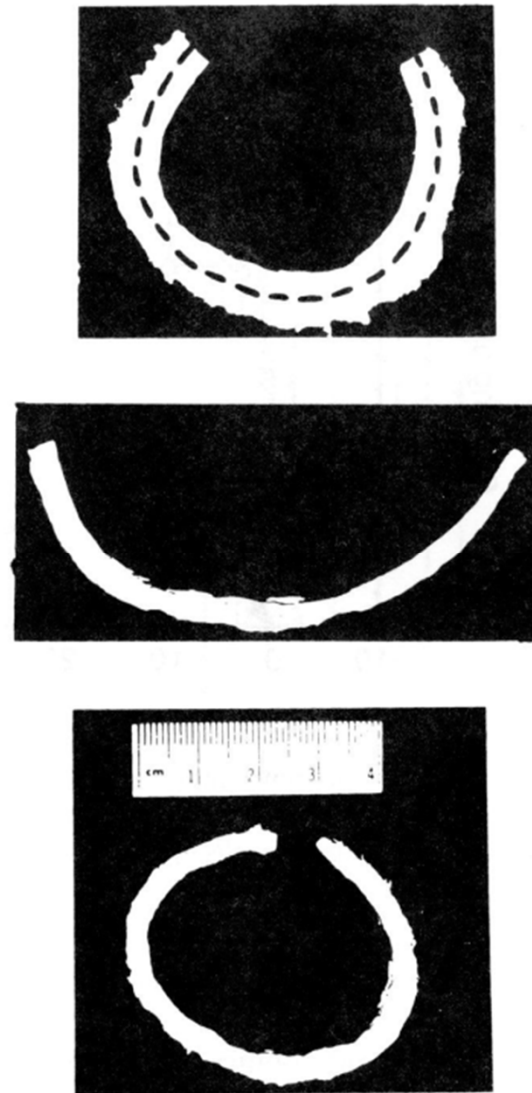


FIGURE 7.13. Opening-up of outer (bottom) and inner (middle) unloaded arterial rings taken from a single (top) arterial cross section. The dashed line shows how the original cut separated the original ring into concentric rings. (From Vossoughi et al, 1993, with permission.)

Humphrey (2002)

How may affect different external conditions and intrinsic phenomena the observed opening angle?

- The opening angle is relatively insensitive to the temperature of the bathing solution (from 25 to 40°C) (Badrek-Amoudi, 1996).
- The opening angle continues to increase for 15 to 30 minutes after cut → the opening is viscoelastic.
- Smooth muscle activity does affect the measured opening angle →

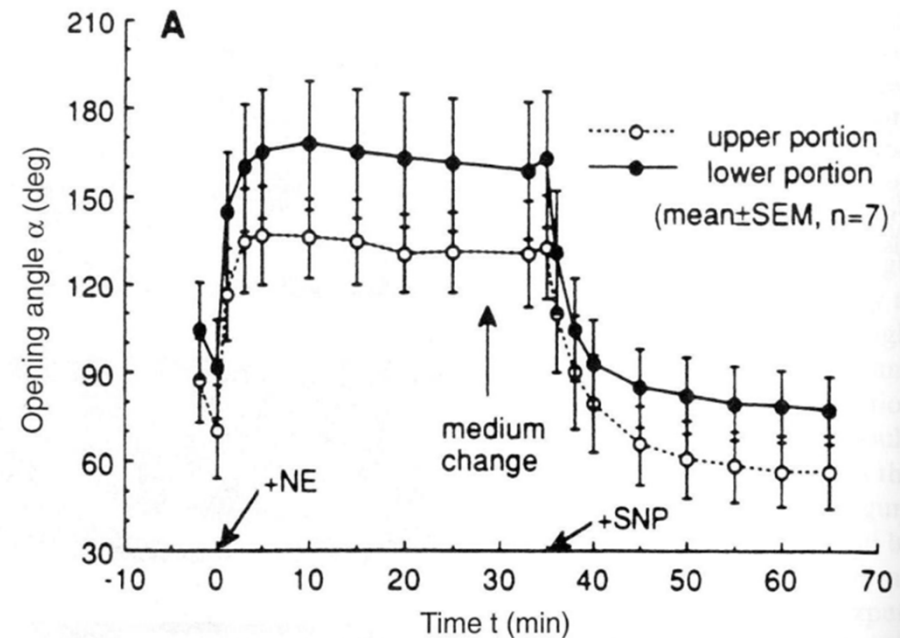


FIGURE 7.14. Opening angle α ($\equiv \Phi_0$) as a function of activation. The vasoconstrictor norepinephrine (NE) was administered at time $t = 0$ and the vasodilator sodium nitroprusside (SNP) at $t = 35$ minutes. (From Matsumoto et al, 1996, with permission.)

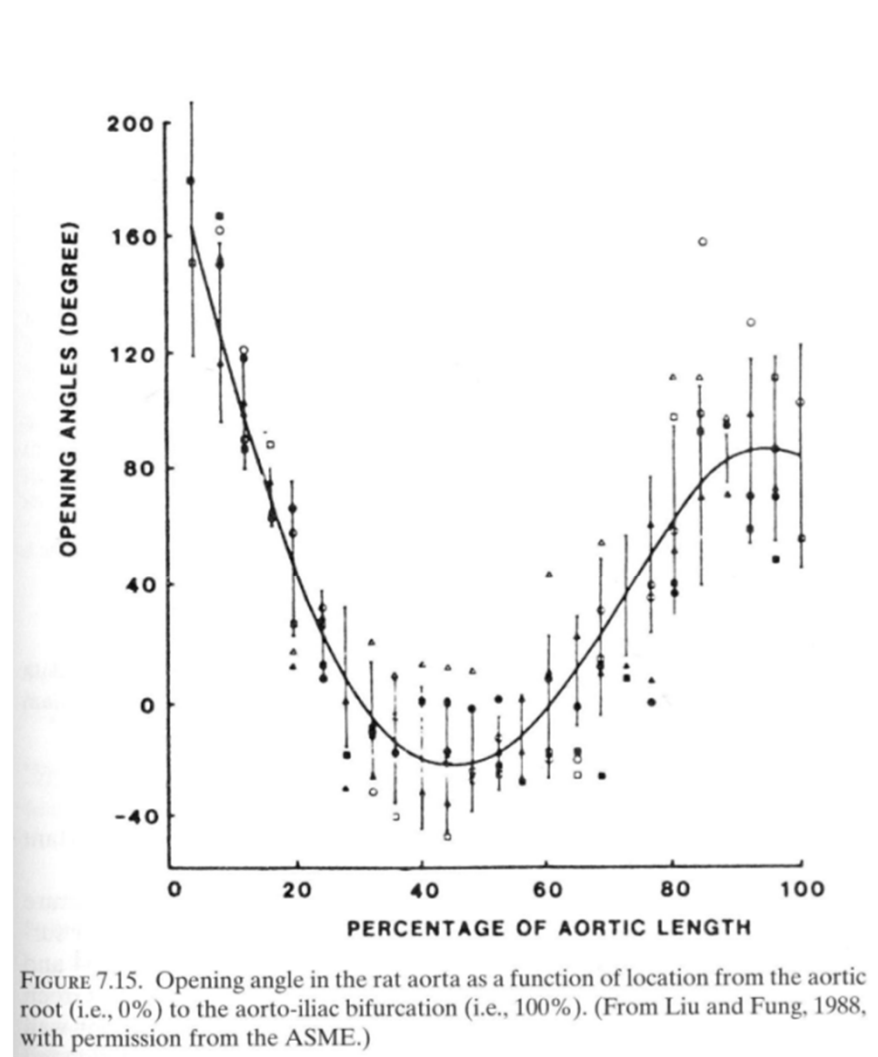


FIGURE 7.15. Opening angle in the rat aorta as a function of location from the aortic root (i.e., 0%) to the aorto-iliac bifurcation (i.e., 100%). (From Liu and Fung, 1988, with permission from the ASME.)

Humphrey (2002)

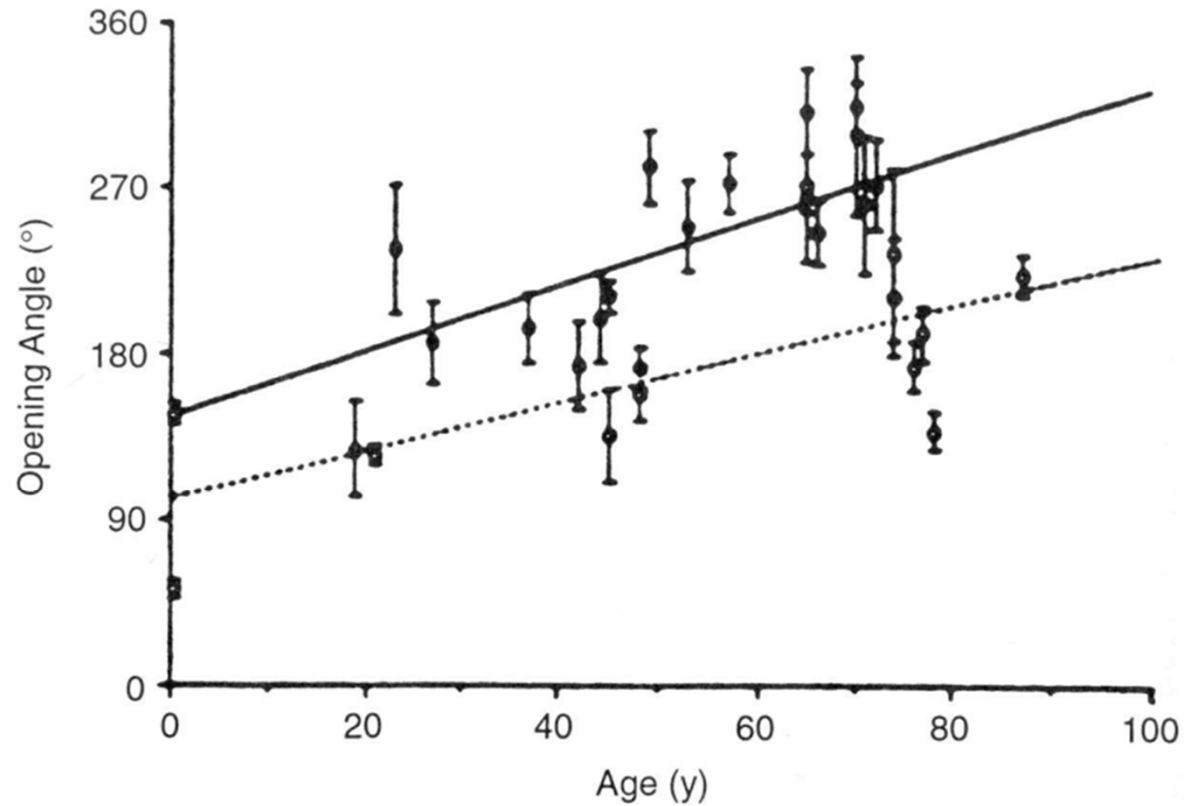
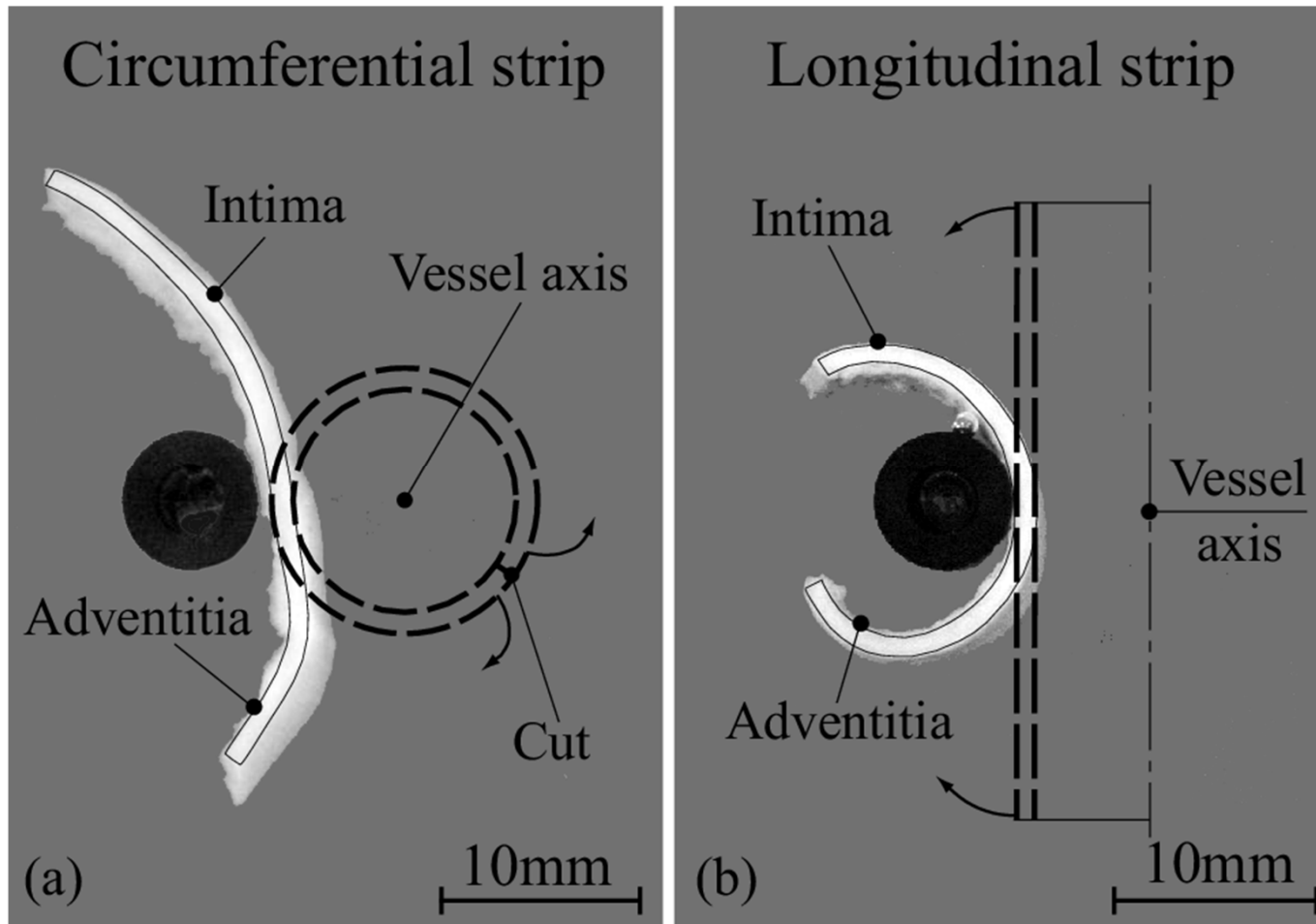


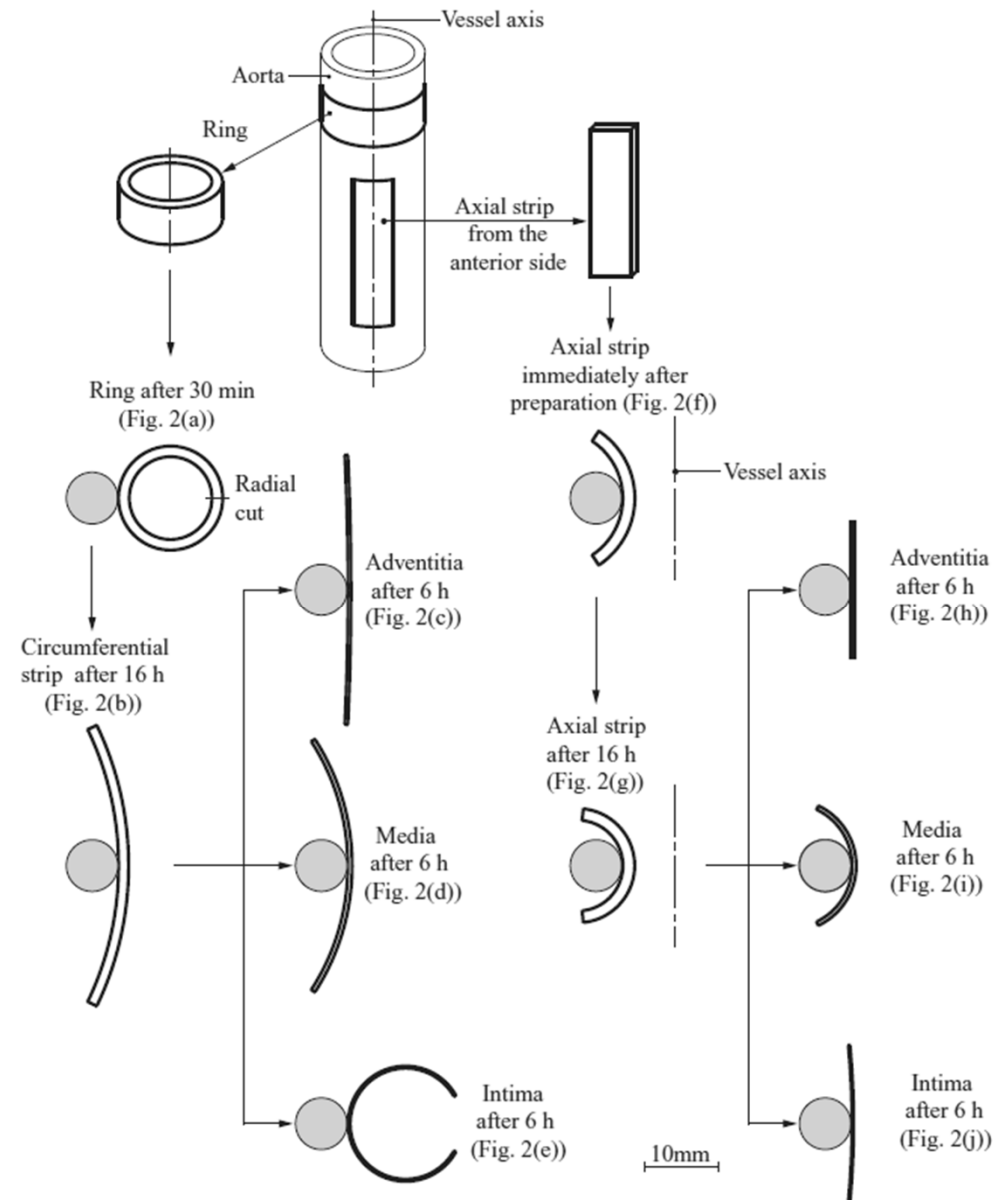
FIGURE 7.16. Effect of age on the opening angle. Closed circles (top line) show data from males and open circles (bottom line) show data from females. (From Sani et al, 1995, with permission, Karger, Basel.)

Layer-Specific 3D Residual Deformations of Human Aortas

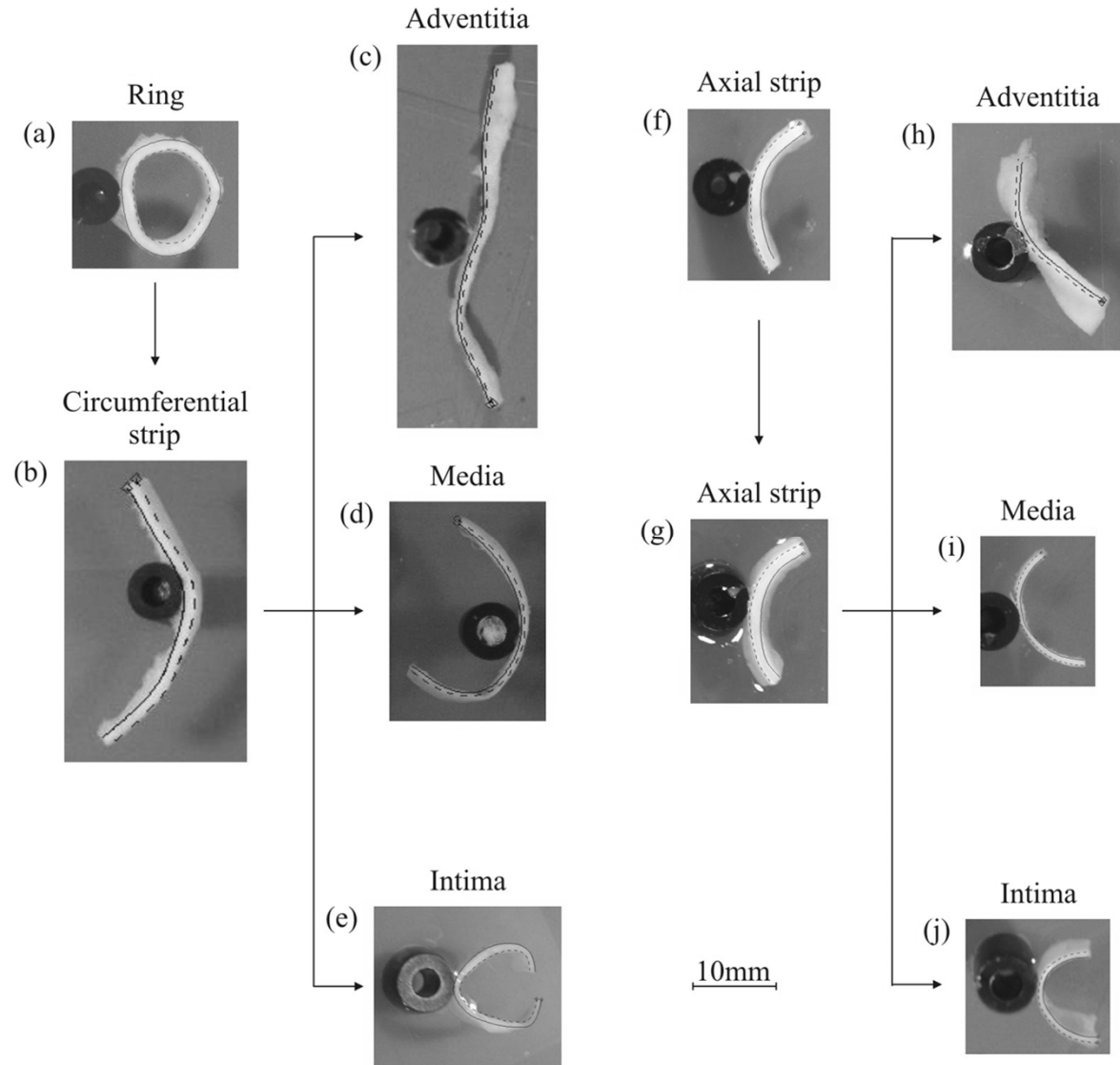
Circumferential and axial strip of an human abdominal aorta



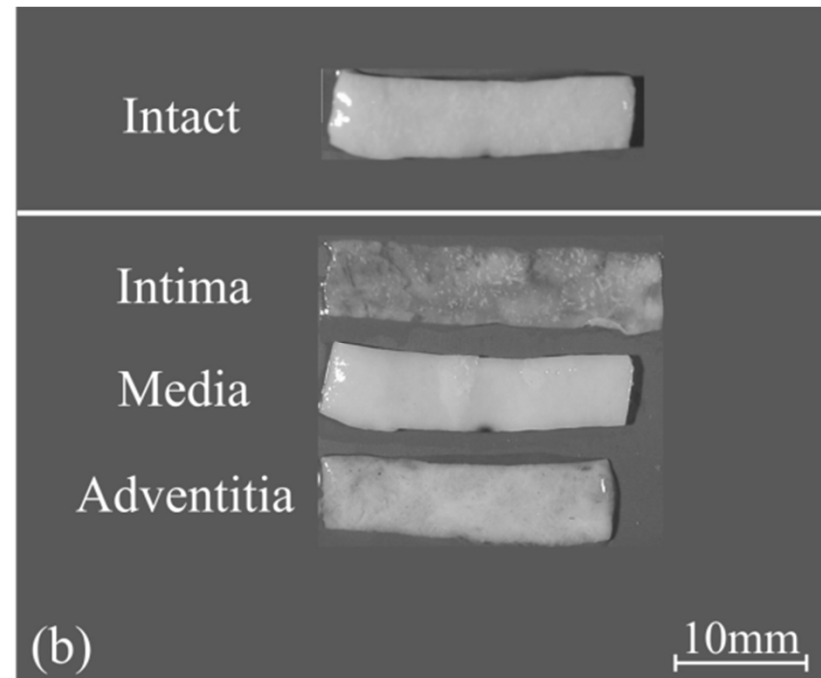
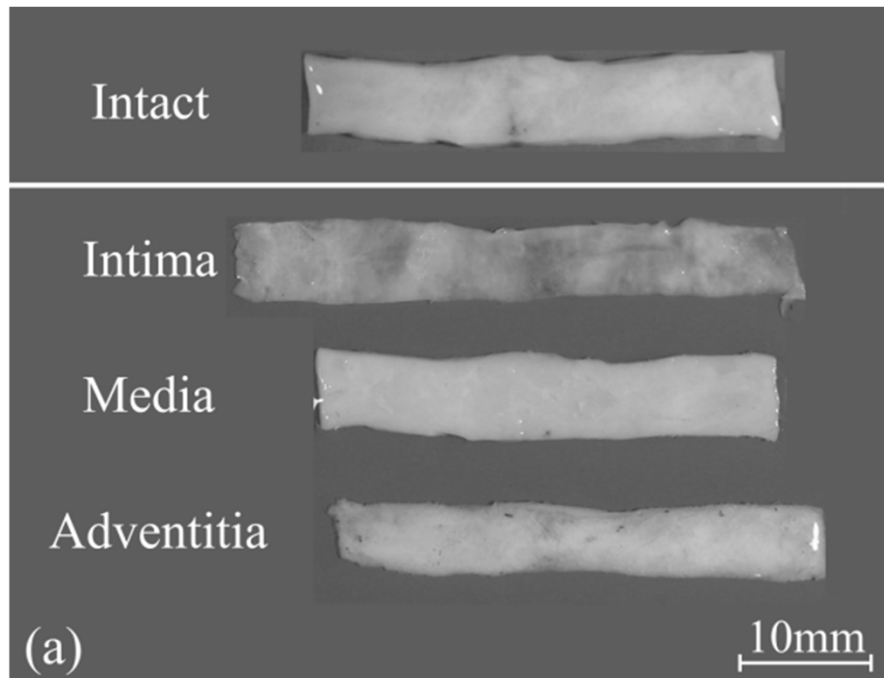
Schematic illustration of the specimen preparation



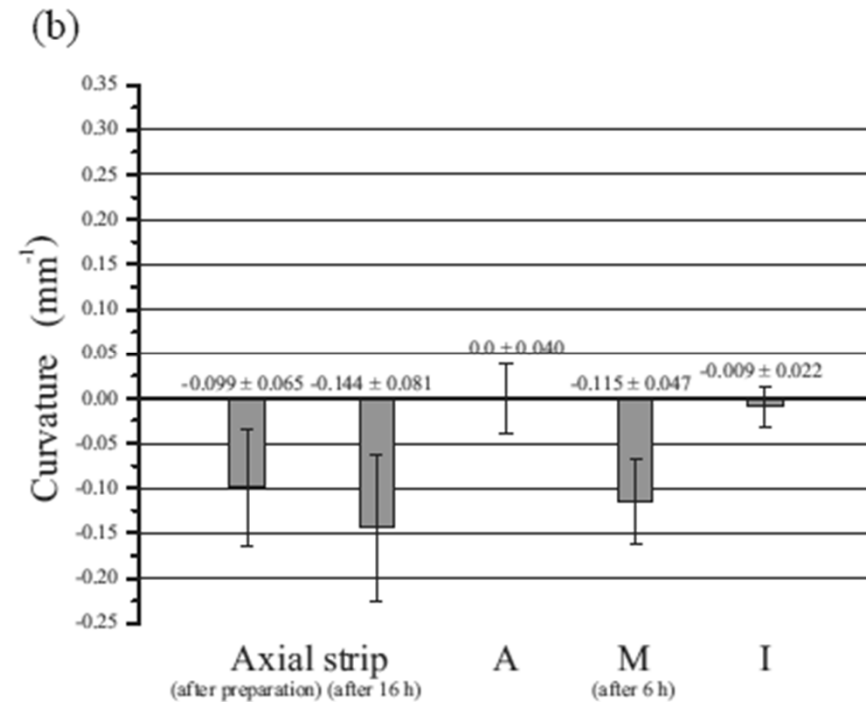
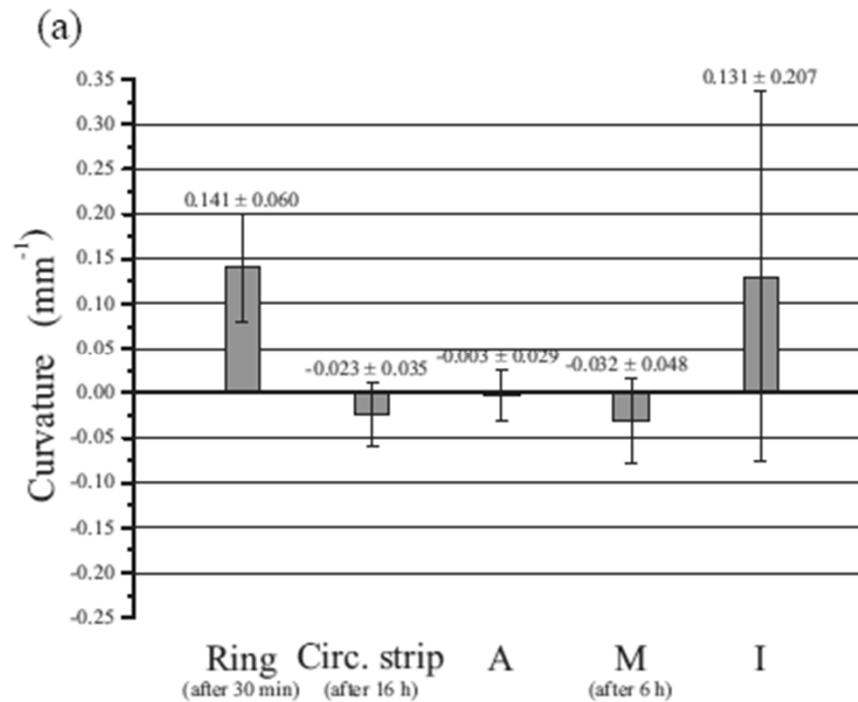
Example of specimens prepared



Length of the strip specimens in the circumferential (left) and axial direction (right)



Results: Curvatures of the aortic specimens



Summary

We observed:

Residual deformations are three dimensional and cannot be described by a single parameter such as 'the' opening angle

It is required to consider both stretching and bending, which are highly layer-specific and direction dependent

Active Response

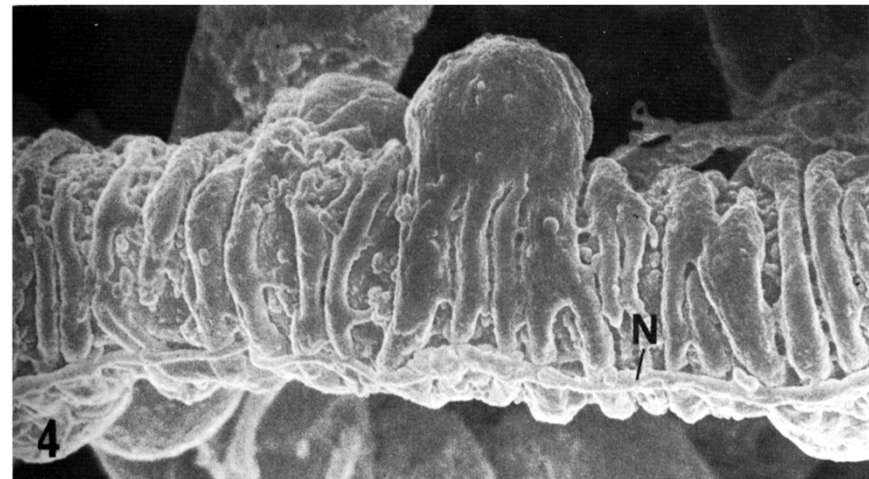
Vascular Smooth muscle governs the luminal area and thereby the local hemodynamics. The response is triggered mechanically (stretch) and biochemically.

Vasodilators

- NO
- histamine

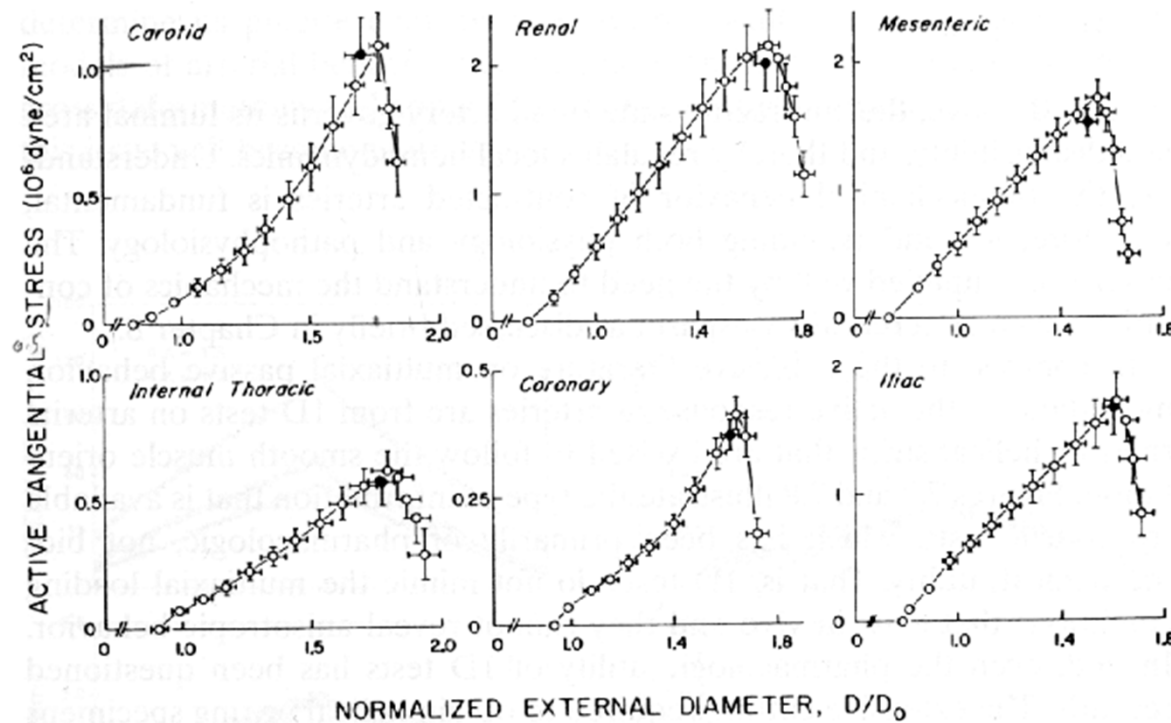
Vasoconstrictors

- Norepinephrine (Noradrenalin)
- Endothelin
- Angiotensin



Scanning electron micrograph of smooth muscle cells surrounding a precapillary arteriole. From Ethier, Simmons [2007]

Active stress in the arterial wall Vascular smooth muscle

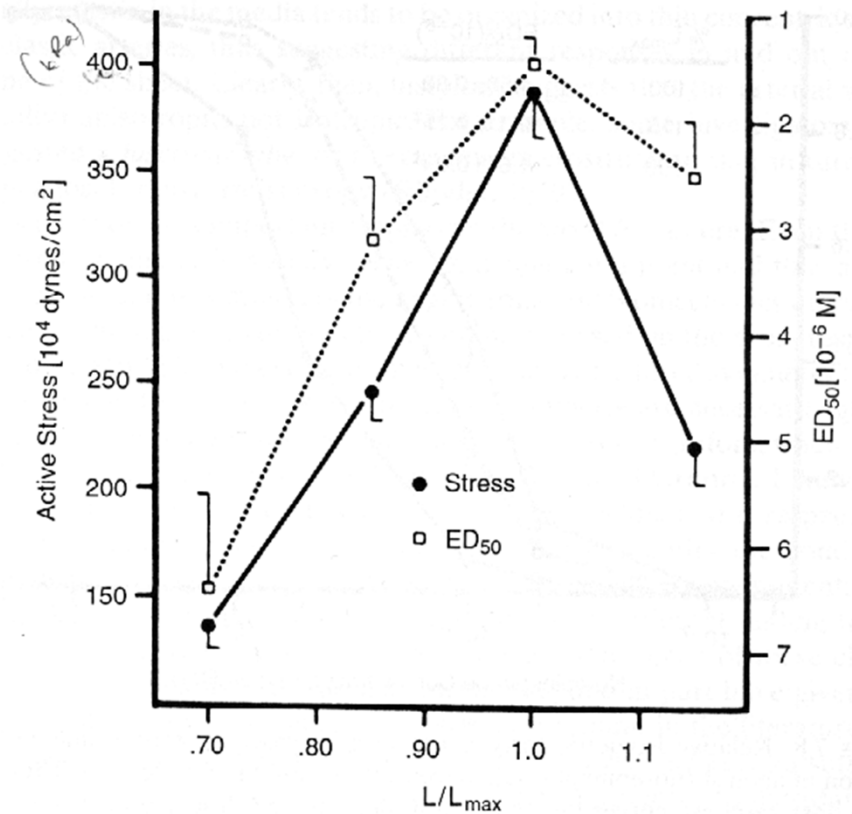


Humphrey (2002)

Active circumferential response of canine arteries.

Force-length behavior

Vascular smooth muscle



Humphrey (2002)

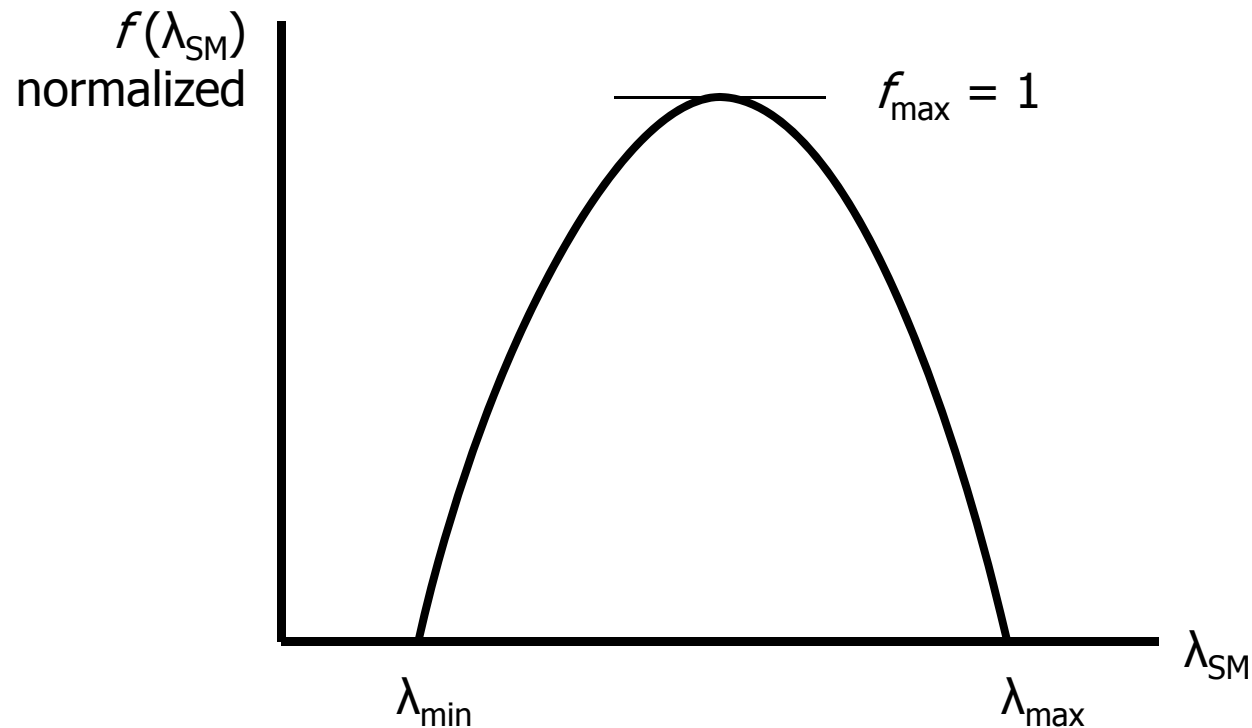
Force-length relation of vascular smooth muscle

L_{max} ... length at maximum force

ED_{50} ... median effective dose of agonist (norepinephrine)

Modeling the force-length behavior

Vascular smooth muscle



Idealized force-length relation of vascular smooth muscle

$$f(\lambda_{SM}) = -\frac{4}{(\lambda_{max} - \lambda_{min})^2} (\lambda_{SM} - \lambda_{min})(\lambda_{SM} - \lambda_{max})$$

Modeling active stress in arteries

Vascular smooth muscle

Active contribution to first Piola-Kirchhoff stress in circumferential direction

$$P_{\theta\theta}^a = S f(\lambda_{SM})$$

S ... maximum stress per unit reference area developed by the smooth muscle cells at a given activation level

f ... normalized, parabolic tension-stretch relationship in the muscle

Recall:

$$\boldsymbol{\sigma}^a = J^{-1} \mathbf{P}^a \mathbf{F}^T$$

